

UV phototransistors based upon spray coated and sputter deposited ZnO TFTs

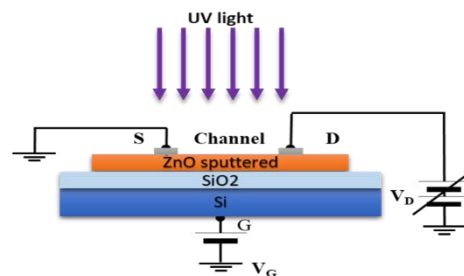
Dinesh Kumar^{1*}, Tiago Carneiro Gomes², Neri Alves², Lucas Fugikawa Santos³, Graham C. Smith⁴ and Jeff Kettle¹

¹School of Electronics, Bangor University, Bangor, Gwynedd, LL57 1UT, Wales, UK.

²São Paulo State University (Unesp), School of Technology and Sciences, Presidente Prudente, Brazil.

³São Paulo State University (Unesp), Institute of Geosciences and Exact Sciences, Rio Claro, Brazil

⁴Faculty of Science & Engineering, University of Chester, Chester CH2 4NU, UK



Abstract— The report of Zinc Oxide (ZnO) phototransistors prepared by spray and sputter coating process is presented. To maximize the sensor response to UV irradiation, a comparison of ZnO films deposited by spray coating and physical vapour deposition is provided and it is shown that spray coated layers provide significant advantages in sensor response. Topographic images of the samples surface shows that there is increase in roughness in spray coated samples indicating increases in grain size, which leads to greater sensor responsivity. X-ray photoelectron spectroscopy (XPS) is used to understand the root cause of the greater UV responsivity. It was observed that sprayed ZnO TFTs are more sensitive to UV radiation due to higher adsorption of oxygen level in spray deposited ZnO films, which is confirmed by XPS data. Responsivity and external quantum efficiency (EQE) of the sprayed ZnO TFT are also evaluated.

Key words— Flexible, ZnO, spray coating, Radio frequency sputtering, detector, TFT, ultraviolet light.

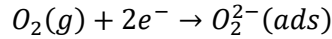
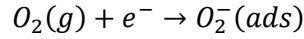
I. Introduction

ZnO and its compounds have generated significant attention since one of their early reports by Nomura et al. in 2004 [1]–[4]. Due to their outstanding electrical properties, such as high field-effect mobility, good uniformity and low temperature processability, ZnO Thin Film Transistors (TFTs) have revealed potential in a wide range of electronic applications like photo detectors [5]–[7]. For example, T. D. Anthopoulos and co-workers demonstrated solution-processed dye-sensitized ZnO phototransistors with high photoresponsivity on the order of 10^4 A/W [8]. Nae-Eung Lee and co-workers reported flexible ultraviolet phototransistor using hybrid channel of vertical ZnO nanorods and graphene showing high-photovoltage responsivity of 10^8 V/W. The benefit of ZnO TFT as phototransistor is that multiple parameters including threshold voltage, mobility and drain ON current changes on exposure to UV radiation. However, in two terminal devices, fewer parameters change giving reduced specificity. In addition, TFTs with tunable threshold voltage, V_{th} , is of particularly high importance for chemical, gas and biological detectors [9].

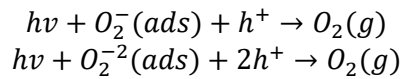
An earlier version of this paper was presented at the FLEPS 2019 (for link please see footnote¹) and was published in its proceedings. Here, we are extending the paper and it will be shown that the photo-transistor UV detector produced by spray pyrolysis are much more responsive for sensor applications rather than those produced by sputter

coating, because they show greater responsivity to UV radiation.

In this work, ZnO TFTs were used for UV photo detection. ZnO is an established candidate for UV detectors because it has a band gap of 3.37 eV [10][11], which corresponds to the UV spectrum. The ZnO active layer conductivity is extremely sensitive to UV radiation exposure, which is related with its photosensitivity regulated by chemisorption of oxygen [12]–[14]. Oxygen molecules can be adsorbed on the surface of ZnO films and extract free electrons from them, resulting in oxygen negatively charged ions that create an electron depletion layer, in which the ZnO layer becomes less conductive near the surface [15]. This process is shown below.



The interaction between UV radiation and ZnO film generates electron-hole pairs. The hole combines with adsorbed oxygen ions in ZnO surface producing oxygen molecules. Under bias condition, the free electrons are collected at the electrode, thereby an increase in conductivity takes place with the decrease in the width of depletion layer formed [16], [17].



In the dark, oxygen is reabsorbed on the surface until the equilibrium is restored again. This reabsorption is a slow process and significantly increases the relaxation time constant of ZnO devices [18]. Both the principle of using ZnO UV photo detection has been well established, enhancements and they haven't been realised by looking at different deposition approaches. In this paper we show how the responsivity is enhanced by modifying the photo active layer structurally by depositing it from spray coating. This also enables the UV detector to be deposited from solution rather than via vacuum processing.

II. EXPERIMENTAL

Spray coating deposition was undertaken using an airbrush nozzle actuated by a micro-controlled servomotor to spray a zinc acetate di-hydrated (3% w/w, in methanol) solution onto pre-heated (300°C) substrates. The substrate heating promotes the solvent evaporation as the solution spray reaches the substrate surface and cause the zinc acetate pyrolysis and subsequent formation of a thin ZnO layer. Spray coating was performed at air pressure 0.7 bar and nozzle kept 20 cm distance from the substrate on hotplate. For optimum film formation, the airbrush nozzle was actuated for three short intervals of 5 seconds within three 60s pause intervals. The resulting ZnO films obtained by this deposition procedure were uniform; with an average thickness of 20 nm. Active layer thickness was determined by Dektak surface profilometer.

ZnO TFTs were also manufactured by using radio frequency (RF) sputtering technique at 75W and 1.2×10^{-2} mbar pressure. The 99.99% pure ZnO target was pre-sputtered under closed shutter for 5 min to remove contaminants from the surface. A low sputter rate of 0.05 nm/s was used for better uniformity and surface roughness of ZnO layer on substrates. ZnO layer thickness during deposition by sputtering was monitored with pre-installed thickness detector on the sputter coater display panel.

For all measurements of IGZO and ZnO TFTs, the electrical properties I_{on} , I_{off} , I_{on}/I_{off} ratio and mobility were extracted from transfer characteristics of TFT using equations (1) and (2).

$$I_{DS} = \mu C_i \frac{W}{2L} (V_{GS} - V_{th})^2 \quad (1)$$

$$\mu_{sat} = \left(\frac{\partial \sqrt{I_D}}{\partial V_G} \right)^2 \frac{2L}{WC_i} \quad (2)$$

where, W is channel width and L is channel length, C_i is dielectric capacitance, μ is carrier mobility, V_G applied gate voltage, V_D is drain voltage, and V_{th} is the TFT threshold voltage.

III. ZNO TFT AS UV PHOTO DETECTOR

A. Transfer characteristics of sprayed and sputtered ZnO TFT under UV light

We have conducted UV photo detection tests on ZnO TFTs manufactured using spray as well as sputtered deposition methods to see the effect of UV irradiation on the TFT characteristics. Fig.1(a) shows transfer characteristics of a ZnO TFT manufactured by spray coating and Fig.1(b) sputter coated before (black curve) and after (in blue) exposure to a UV-355 nm LED for 5 minutes at an irradiance of 0.214 mW/mm². In both cases, the characteristics changed dramatically and shown is the behaviour after 5 minutes of light exposure, by which time the devices had saturated in terms of their electrical changes. Such behaviour is commonly known as “persistent photoconductivity”. This effect can be attributed to the generation of the photo excited carrier concentration in the degenerate level, which changes the behavior of the ZnO from semiconducting to conducting [19].

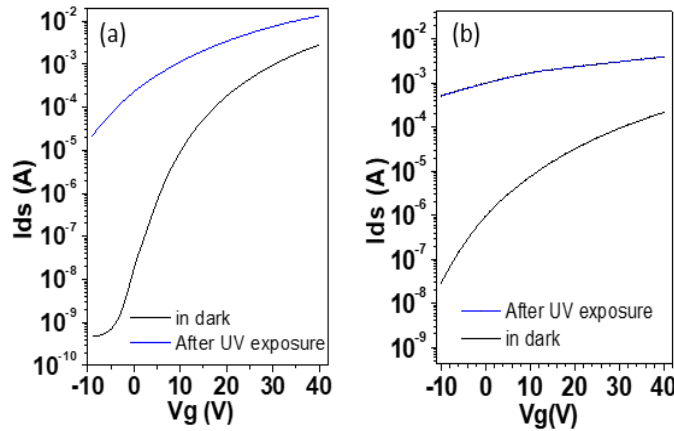


Fig. 1. Transfer curves for a ZnO TFT with the active layer deposited by (a) spray-coating, (b) sputtered before and after UV exposure for 5 minutes at an irradiance of 0.214 mW/mm².

The ZnO TFT performance parameters including mobility, V_{th} and on-off ratio were evaluated before and after exposure UV light. Both types of TFTs show an overall increase in these parameters after UV exposure, however, with more accentuated effect in the in the “off-current” region, where the gate bias is smaller than the threshold voltage. The relative change in these performance parameters is higher in case of sprayed TFTs, suggesting sprayed TFTs are more sensitive for UV irradiation. This can be attributed to higher surface roughness in case of sprayed as confirmed by AFM data (discussed later in Table 5), increased surface area might be responsible to higher adsorption of molecular oxygen to the film surface as confirmed by XPS data (discussed later in Table1 and 3). This increased conductivity effect occurs due to the photo-stimulated desorption of adsorbed oxygen molecules in the ZnO film. In the absence of UV light, oxygen molecules can be adsorbed on the surface as negatively charged ions by capturing the free electrons from the n -type semiconductor, thereby create a depletion layer with low conductivity near the surface. When the sample is exposed to UV light with photon energy in the UV, it generates electron-hole pairs which result in increase in conductivity.

Shown in Fig.2 (a), (d) saturation mobility, (b), (e) and TFT OFF-current (c), (f) TFT on-current shows the decay behaviour of sprayed (left), sputtered (right) the TFT with respect to time elapsed after the UV excitation was switched off for temperatures varying from 40 °C until 102 °C. The mobility for sprayed TFT increases with temperature and presents a slow decay time at 40 °C, however the sputtered TFTs shows similar mobility values at all temperatures of measurements. By increasing the temperature, the decay of the photo-stimulated mobility

becomes faster and nearly no temperature dependence on the curves can be observed. The sprayed TFT on-current Fig.2 (c), however, presents a larger variation, with a faster decay than the carrier mobility, Fig.2 (a), at low temperature (40 °C) and almost invariant behaviour at higher temperatures (above 75 °C), indicating that the on current increase is not only due to the increase in the carrier mobility by UV illumination, but also by the increase in the free charge carrier density in the transistor channel due to elevated temperature excitation energy. The off-current, which is a direct measure of the ZnO film conductivity, presents an even higher variation with temperature and a faster time decay, Fig.2(b), at lower temperatures. The initial value of the off-current is strongly dependent on the temperature, however, for temperatures above 75 °C, a temperature dependence cannot be observed for longer times.

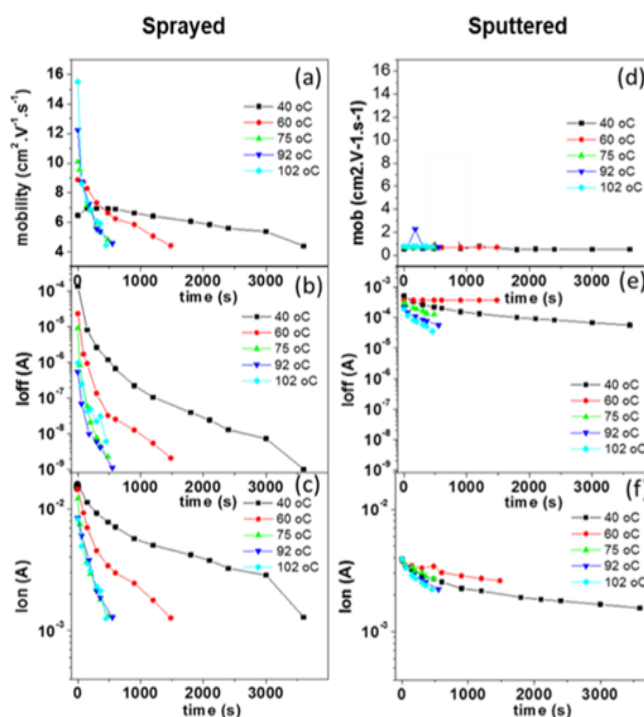


Fig. 2. Decay time of the sprayed ZnO TFT (a) mobility, (b) OFF-current, (c) Drain on-current and sputtered ZnO TFT (d) mobility, (e) off-current, (f) on-current at different temperatures.

From the observed results, we can confirm that, even though the increase on the temperature causes an increase on the UV-stimulated carrier mobility, it is also responsible for accelerating the adsorption of the oxygen molecules to the ZnO TFT active layer, which contributes to the decrease in the carrier mobility and in the semiconductor conductivity. The TFT off-current has a faster decay time than the on-current because the contribution to the off-current comes from the conductivity of the whole ZnO layer, which has a larger area for oxygen adsorption, whereas the contribution to the on-current comes from the conductivity of the ZnO/dielectric interface, which represents a small portion of the whole ZnO film.

Fig.3 shows the temperature dependence of the sprayed TFT mobility (a), and of sputtered ZnO TFT mobility (b), immediately after the UV light was switched off. The TFT mobility increases with temperature, with an activation energy of about 140 meV for sprayed and 53 meV for sputtered TFTs. The density of free carriers (proportional to the TFT off current) can be expressed as equation (3), where, ΔE is the activation energy of the adsorption process.

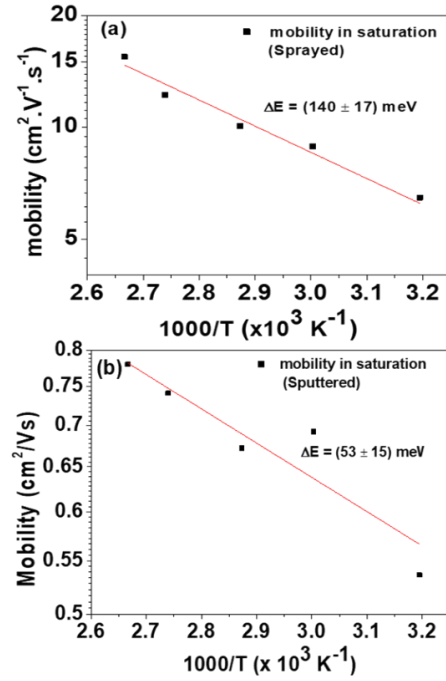


Fig. 3. Temperature dependence of the sprayed TFT mobility (a), and of sputtered ZnO TFT mobility (b) immediately after the UV light was switched off.

$$n = n_0 \left[1 - \exp\left(-\frac{\Delta E}{k_B T}\right) \right] \quad (3)$$

This equation was used to calculate activation energy. This behavior dependent of temperature is dominated more by thermal excitation of electrons than absorption/desorption of oxygen molecules in surface of the ZnO film, which may arise due to native defects such as interstitial zinc atoms and oxygen vacancies. The I_{off} current decreases due to the adsorption of oxygen molecules to the ZnO film. However, this process is strongly dependent of the temperature to sprayed ZnO films, since that it has very low thermal activation energy, but there is little influence of the temperature on the sputtered ZnO films, as activation energy is much higher. Overall the results show that the sputtered samples are less sensitive to UV irradiation as compared to sprayed because charge transfer in sputtered is quicker.

Overall, the higher UV sensitivity in case of sprayed as compared to sputtered TFTs is attributed to higher oxygen level in as prepared as well as annealed samples (as confirmed by XPS data).

B. Responsivity and external quantum efficiency of the sprayed ZnO TFT

An important parameter to evaluate the performance of the radiation detectors is the responsivity and external quantum efficiency (EQE). Responsivity and EQE of sprayed ZnO TFTs were evaluated at three different wavelengths ($\lambda = 355\text{nm}, 370\text{nm}, 385\text{ nm}$) and shown in Fig. 4(a) and 4(b). The measurement was carried out from transfer curve at $V_{\text{DS}} = 40\text{V}$ at room temperature in air. These properties are given, respectively, by equations (4) and (5) [20]:

$$\text{Responsivity} = \frac{I_{\text{total}} - I_{\text{dark}} / A_{\text{pt}}}{P / A_{\text{pd}}} = \frac{J_{\text{ph}}}{P} \quad (4)$$

$$\text{EQE} = \frac{J_{\text{ph}} / q}{P / h\nu} \quad (5)$$

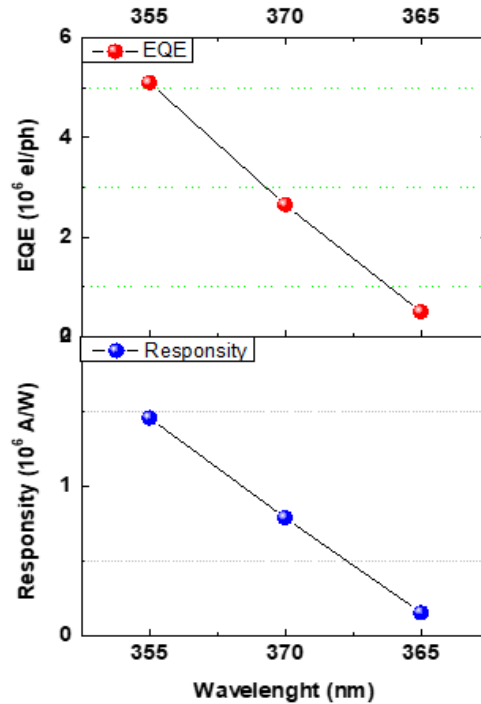


Fig. 4. (a) EQE and (b) responsivity evaluated at different laser wavelengths ($\lambda = 355\text{nm}$, 370nm and 385 nm)

Both responsivity and EQE exhibited a linear relation with wavelength for both sprayed and sputtered ZnO TFT. The highest values of the responsivity and EQE were obtained with 355nm wavelength, which are $1.46 \times 10^6\text{ A/W}$ and $5.1 \times 10^6\text{ el/ph}$, respectively. Both responsivity and EQE values were increased because higher the photon energy region, the ZnO films absorb more photons and hence the number of carriers in conduction band increases, which leads to increase in the photocurrent. This value of responsivity is better as compared to another reported works. For example, Guo, *et al*, manufactured photoconductors based on transistor with mechanically exfoliated single layer of Graphene/ZnO QDs, which displayed responsivity of 10^4 A/W at UV wavelength of 325 nm and $V_{DS} = 1\text{mA}$ [21]. Dang, *et al*, showed that the maximum responsivity the ZnO Nanorods/Graphene hybrid FET under UV light at 365 nm wavelength was $3 \times 10^5\text{ A/W}$ for transistors at $V_{DS} = 1\text{ V}$ [22].

Evidently the responsivity depends on strongly of the kind device, UV wavelength, composition, structure and morphology of material as well as of the V_{DS} applied in case to use detector based on transistor. However, our ZnO TFT, with large channel ($L=400\mu\text{m}$) and measured at room temperature in air showed promising results for responsivity and EQE.

IV. XPS ANALYSIS OF ZNO FILMS

X-ray photoelectron spectroscopy (XPS) was performed on both sputtered and sprayed ZnO TFTs to see the effects of UV light on ZnO TFT photodetector. From XPS data analysis, the samples consisted of near-pure stoichiometric ZnO with a hydrocarbon overlayer due to absorption from the environment, as is usually seen in XPS analysis of air-exposed samples. Annealing did not appear to change the chemistry or stoichiometry of the ZnO; however, it did result in a reduction in the amount of hydrocarbon contamination. If the hydrocarbon was assumed to be present as a uniform thin overlayer, then its thickness was reduced from approximately 1.75 nm to approximately 1.15 nm on annealing. For spray-coated films, where hydrocarbon contamination did not play an important role, annealing seemed to change slightly the sample chemistry and stoichiometry, leading to a higher amount of oxygen in metallic

bonds in the crystalline lattice and a higher amount of oxygen vacancies, leading to more UV light sensitivity of sprayed TFTs.

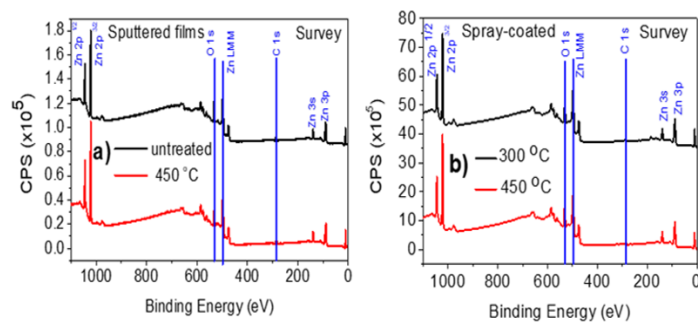


Fig. 5. XPS survey scans from sputtered (a) and spray-coated ZnO films.

XPS spectra from all samples (both sputtered and sprayed) showed strong Zn and O peaks, with C also present. The annealed sputtered sample also showed a very low level of Cl. As an example, the survey scan for the as-prepared sputtered sample is shown in Figure 5(a) and for the spray-coated films, in Figure 5(b). The results of quantification of the data are shown in Table 1.

The data shows that annealing of the sputtered films reduced the amount of surface carbon present and also reduced the ratio of oxygen to zinc from ~ 1.7 to ~ 1.4 . Stoichiometric ZnO is expected to show a ratio of O/Zn of 1. The difference is probably due to preferential attenuation of the Zn $2p_{3/2}$ signal compared to the O 1s signal by the surface carbonaceous overlayer, as a consequence of the lower kinetic energy of the Zn $2p_{3/2}$ photoelectrons. To correct the measured surface compositions for the effect of the hydrocarbon overlayer, the method of Smith (2005) was applied. In this method, the carbon composition is used to estimate the thickness of the hydrocarbon contamination overlayer, the effect of a layer of this thickness on the attenuation of signals from the underlying material is estimated, and the results are re-normalised to 100 atom %. The results of applying this correction for sputtered samples are shown in Table 2.

TABLE 1. SURFACE COMPOSITION FOR SPUTTERED AND SPRAY-COATED ZNO FILMS

Element	Position [eV]	Surface concentration, atom %			
		Sputtered Films		Spray-coated films	
		As-prepared	Annealed	300 [°C]	450 [°C]
C 1s	284.8	39.12	27.79	22.75	22.53
O 1s	530	38.59	42.33	48.07	48.69
Zn $2p_{3/2}$	1022	22.29	29.71	29.18	28.77
Cl 2p		-	0.16	-	-

The results show a much closer approach to the stoichiometric ZnO, as expected, but a smaller Zn content in the spray coated film, indicating a lower level of C impurities. The slight excess of O is most likely due to the presence of some carbon-bonded oxygen. Hydrocarbon contamination in spray-coated films was not so significant and the correction procedure was not applied.

TABLE 2. SURFACE COMPOSITIONS AFTER APPLICATION OF THE HYDROCARBON CONTAMINATION OVERLAYER CORRECTION

		As prepared	Annealed
Hydrocarbon layer thickness (nm):		1.75	1.15
Element and line	O 1s	52.94	51.78
	Zn 2p ^{3/2}	47.06	48.22
Ratio O/Zn		1.13	1.07

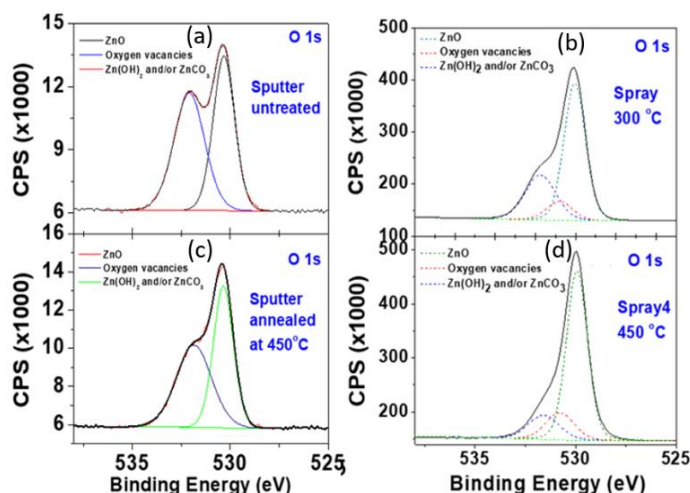


Fig. 6. (a) Sputtered untreated high-resolution spectra for O 1s, (b) sputtered annealed at 450 °C high-resolution spectra for O 1s (c) sprayed at 300 °C high-resolution spectra for O 1s (d) sprayed at 450 °C high-resolution spectra for O 1s.

High resolution scans over the O1s peaks (for sputtered and sprayed samples) are shown in Fig.6 also, curve-fitted to known chemical state reference data. The spectra from the sputtered films show a strong component at approximately 530.4 eV and a broader component at approximately 532 eV. The sharper component at lower binding energy is attributed to oxygen in metallic bonds (in ZnO in this case), with the broader component at higher binding energy due to oxygen in a range on unresolved carbon bonding configurations, consistent with those observed in the C 1s peak. The difference between as-prepared and annealed samples is consistent with the reduction in the hydrocarbon contamination layer (and its associated oxygen bonds) on annealing.

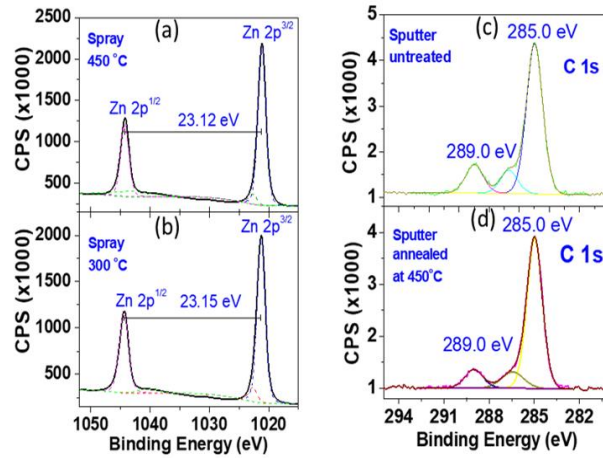


Fig. 7. (a) Zn 2p spectra for spray-coated films annealed at 450 °C, (b) Zn 2p spectra for spray-coated films annealed at 300 °C, Carbon 1s spectra for sputtered samples (c) untreated, (d) annealed at 450 °C.

TABLE 3. COMPONENT ASSIGNMENT FOR THE O 1S SPECTRA FROM THE SPRAY-COATED SAMPLES.

Component	Spray Annealed at 300 [°C]		Spray Annealed at 450 [°C]	
	Position	%At Concentration	Position	%At Concentration
O 1s (a)	530.04	60.81	529.93	69.69
O 1s (b)	530.80	10.47	530.79	15.40
O 1s (c)	531.75	28.73	531.58	14.91

High resolution scans over the C 1s peaks from sputtered samples are shown in Fig.7, curve-fitted to known chemical state reference data. Both C 1s spectra show strong hydrocarbon peaks at 285.0 eV, with weaker components at approximately 286.5 eV and 289.0 eV due to C-O (hydroxyl) and COO- (surface acid groups). After annealing, there was a small drop in the relative proportion of acid groups compared to the non-annealed samples (11% of the C 1s intensity, compared to 15% of the C 1s intensity as prepared). However, any differences in chemical state after annealing were minor. Similar peaks (but less intense) were observed in spray-coated samples (HR scans not shown).

Spray-coated films had much narrower O1s spectra, probably due to the longer annealing time (1 hour). The spectra were fitted considering three major contributions, as shown in Table 3. The low-energy and more intense component at 530 eV is attributed to oxygen in metallic bonds, forming crystalline ZnO. Two smaller components are observed at 530.8 eV and 531.7 eV. The higher energy component can be attributed to oxygen in ZnOH or ZnCO₃ bonds, since the spray-coated ZnO films are formed by the pyrolysis of an organic precursor salt, zinc acetate dihydrate. The intermediate component at 530.8 eV is commonly attributed to oxygen atoms in oxygen deficient regions caused by oxygen vacancies [23]. Table 3 shows that the annealing at 450 °C increased the amount of oxygen in the crystalline lattice, simultaneously by the decrease of the amount of oxygen in ZnOH and ZnCO₃, which is consistent with the picture of higher conversion from zinc acetate to ZnO. Moreover, the increase of the amount of oxygen related to oxygen vacancies for the annealed sample is in agreement with the observed improvement of the electrical properties of the films, since the n-type conductivity of ZnO can be associated to oxygen vacancies [24].

V. ATOMIC FORCE MICROSCOPY OF ZNO FILMS

AFM topography images of ZnO films prepared using spray and sputter deposition techniques are shown in in Fig.8. However, there is very small increase in roughness at higher temperature of annealing for both sputtered as well spray deposited films. The surface roughness of the films was evaluated in terms of root mean square (R_q), average (R_a) and peak to valley (R_{max}) and are shown in Table 5. This small increase in roughness can be attributed to increases in grain sizes, which can be verified from the AFM images in Fig.8.

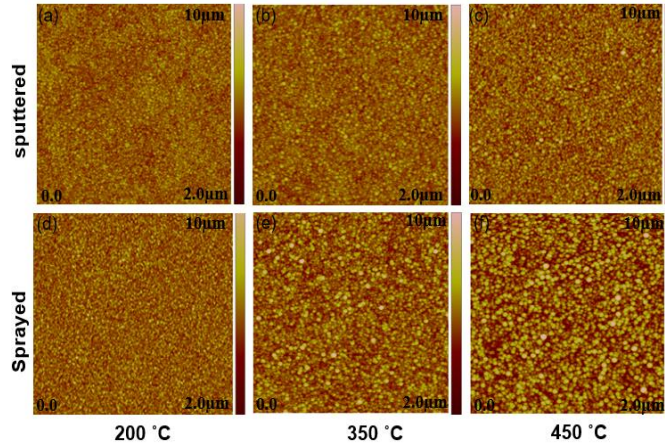


Fig. 8. (a), (b), (c) sputtered AFM topography images of sputtered and (d), (e), (f) sprayed ZnO films annealed at different temperatures shown above.

TABLE 5. SURFACE ROUGHNESS PARAMETERS OF SPRAYED AND SPUTTERED ACTIVE LAYERS OF ZNO TFTS

Annealing T (°C)	Sprayed Roughness Parameters			Sputtered Roughness Parameters		
	R _q (nm)	R _a (nm)	R _{max} (nm)	R _q (nm)	R _a (nm)	R _{max} (nm)
200	1.43	1.09	14.3	0.60	0.48	5.30
350	1.51	1.15	14.6	0.62	0.49	5.40
450	1.96	1.55	17.6	0.74	0.56	11.15

VI. CONCLUSION

The effect of UV light on ZnO photo transistors prepared by spray pyrolysis and sputtering has been investigated. It was demonstrated that sprayed ZnO TFTs are more sensitive to UV light as compared to sputtered TFTs. This is due to higher oxygen level in sprayed ZnO TFTs and is confirmed by XPS data. Higher oxygen level in sprayed ZnO TFTs can be attributed to higher surface roughness in case of sprayed as confirmed by AFM data, increased surface area might be responsible to higher adsorption of molecular oxygen to the film surface and this was confirmed by XPS analysis.

ACKNOWLEDGMENT

We acknowledge the technical support from the Nanostructured Soft Materials Laboratory, LNNano-CNPEN, Brazil (XPS-23205 proposal) for XPS measurements and the Nanotechnology National Laboratory for Agriculture (LNN/EMBRAPA) supported by CNPq/SISNANO/MCTI for XRD measurements. JK and DK would like to thank the Welsh European Funding Office (WEFO) for funding the 2nd Solar Photovoltaic Academic Research Consortium (SPARC II)

REFERENCES

- [1] K. Nomura, H. Ohta, A. Takagi, T. Kamiya, M. Hirano, and H. Hosono, "Room-temperature fabrication of transparent flexible thin-film transistors using amorphous oxide semiconductors," *Nature*, vol. 432, no. 7016, pp. 488–492, 2004.
- [2] H. C. You and C. J. Wang, "Low-temperature, solution-processed, transparent zinc oxide-based thin-film transistors for sensing various solvents," *Materials (Basel)*, vol. 10, no. 3, 2017.
- [3] S. Vishniakou *et al.*, "Improved Performance of Zinc Oxide Thin Film Transistor Pressure Sensors and a Demonstration of a Commercial Chip Compatibility with the New Force Sensing Technology," *Adv. Mater. Technol.*, vol. 3, no. 3, pp. 1–9, 2018.
- [4] M.-H. Hsu, S.-P. Chang, S.-J. Chang, C.-W. Li, J.-Y. Li, and C.-C. Lin, "Fabrication of Zinc Oxide-Based Thin-Film Transistors by Radio Frequency Sputtering for Ultraviolet Sensing Applications," *J. Nanosci. Nanotechnol.*, vol. 18, no. 5, pp. 3518–3522, 2017.
- [5] M. H. Hung *et al.*, "Ultra low voltage 1-V RFID tag implement in a-IGZO TFT technology on plastic," *2017 IEEE Int. Conf. RFID, RFID 2017*, pp. 193–197, 2017.
- [6] W. Cai *et al.*, "One-Volt IGZO Thin-Film Transistors with Ultra-Thin, Solution-Processed Al_xO_y Gate Dielectric," *IEEE Electron Device Lett.*, vol. 39, no. 3, pp. 375–378, 2018.
- [7] B. Kim *et al.*, "A depletion-mode a-IGZO TFT shift register with a single low-voltage-level power signal," *IEEE Electron Device Lett.*, vol. 32, no. 8, pp. 1092–1094, 2011.
- [8] P. Pattanasattayavong, S. Rossbauer, S. Thomas, J. G. Labram, H. J. Snaith, and T. D. Anthopoulos, "Solution-processed dye-sensitized ZnO phototransistors with extremely high photoresponsivity," *J. Appl. Phys.*, vol. 112, no. 7, 2012.
- [9] J. Sun, J. Jiang, A. Lu, W. Dou, B. Zhou, and Q. Wan, "Low-voltage oxide-based TFTs self-assembled on paper substrates with tunable threshold voltage," *IEEE Trans. Electron Devices*, vol. 59, no. 2, pp. 380–384, 2012.
- [10] T. Ohshima, T. Ikegami, K. Ebihara, and R. K. Thareja, "Photo-excited photonic characteristics of ZnO thin films deposited by laser ablation method," *Electr. Eng. Japan (English Transl. Denki Gakkai Ronbunshi)*, vol. 144, no. 3, pp. 1–7, 2003.
- [11] L.-N. Nguyen, W.-H. Chang, C.-D. Chen, and Y.-W. Lan, "Superior phototransistors based on a single ZnO nanoparticle with high mobility and ultrafast response time," *Nanoscale Horizons*, 2019.
- [12] S. K. Shaikh, V. V. Ganbavle, S. I. Inamdar, and K. Y. Rajpure, "Multifunctional zinc oxide thin films for high-performance UV photodetectors and nitrogen dioxide gas sensors," *RSC Adv.*, vol. 6, no. 31, pp. 25641–25650, 2016.
- [13] S. P. Ghosh *et al.*, "Ultraviolet photodetection characteristics of Zinc oxide thin films and nanostructures," *IOP Conf. Ser. Mater. Sci. Eng.*, vol. 115, no. 1, 2016.
- [14] H. Minoura, Y. Ohya, M. Kanamori, A. Kondoh, and Y. Takahashi, "Photoconductivity of Ultrathin Zinc Oxide Films," *Jpn. J. Appl. Phys.*, vol. 33, no. Part 1, No. 12A, pp. 6611–6615, 2002.
- [15] S. Mansouri, R. Bourguiga, and F. Yakuphanoglu, "Analytic model for ZnO-thin film transistor under dark and UV illumination," *Curr. Appl. Phys.*, vol. 12, no. 6, pp. 1619–1623, 2012.
- [16] D. A. Melnick, "Zinc oxide photoconduction, an oxygen adsorption process," *J. Chem. Phys.*, vol. 26, no. 5, pp. 1136–1146, 1957.
- [17] G. Chai, O. Lupan, L. Chow, and H. Heinrich, "Crossed zinc oxide nanorods for ultraviolet radiation detection," *Sensors Actuators, A Phys.*, vol. 150, no. 2, pp. 184–187, 2009.
- [18] P. Ivanoff Reyes, C. J. Ku, Z. Duan, Y. Xu, E. Garfunkel, and Y. Lu, "Reduction of persistent photoconductivity in ZnO thin film transistor-based UV photodetector," *Appl. Phys. Lett.*, vol. 101, no. 3, 2012.
- [19] D. Li, L. Zhao, R. Wu, C. Ronning, and J. G. Lu, "Temperature-dependent photoconductance of heavily doped ZnO nanowires," *Nano Res.*, vol. 4, no. 11, pp. 1110–1116, 2011.
- [20] S. W. Shin, K. H. Lee, J. S. Park, and S. J. Kang, "Highly Transparent, Visible-Light Photodetector Based on Oxide Semiconductors and Quantum Dots," *ACS Appl. Mater. Interfaces*, vol. 7, no. 35, pp. 19666–19671, 2015.
- [21] W. Guo, S. Xu, Z. Wu, N. Wang, and M. M. T. Loy, "Oxygen-Assisted Charge Transfer Between ZnO Quantum Dots and Graphene," *Small*, vol. 9, no. 18, pp. 3031–3036, 2013.
- [22] V. Q. Dang, T. Q. Trung, and B. Hwang, "Ultrahigh Responsivity in Graphene – ZnO Nanorod Hybrid UV Photodetector," *Small*, vol. 11, no. 25, pp. 3054–3065, 2015.

-
- [23] Y. Tu *et al.*, "Control of oxygen vacancies in ZnO nanorods by annealing and their influence on ZnO/PEDOT:PSS diode behaviour," *J. Mater. Chem. C*, vol. 6, no. 7, pp. 1815–1821, 2018.
- [24] L. Liu *et al.*, "Oxygen vacancies : The origin of n -type conductivity in ZnO," vol. 235305, pp. 1–6, 2016.